

# (Cyclopentadienyl)lanthanide Compounds $\text{Ln}(\text{C}_5\text{Me}_5)_2$ (Ln = Sm, Eu, Yb): Photoelectron Spectra and Molecular Orbital Calculations

Jennifer C. Green\*

*Inorganic Chemistry Laboratory, South Parks Road, Oxford OX1 3QR, England*

Detlef Hohl and Notker Rösch\*

*Lehrstuhl für Theoretische Chemie, Technische Universität München, D-8046 Garching, Federal Republic of Germany*

Received July 17, 1986

Vapor-phase He I and He II photoelectron spectra have been obtained for monomeric  $\text{Ln}(\text{C}_5\text{Me}_5)_2$  (Ln = Sm, Eu, Yb). Quasi-relativistic SCF- $X\alpha$ -scattered-wave calculations of the model systems  $\text{Ln}(\text{C}_5\text{H}_5)_2$  (Ln = Eu, Yb) are presented to analyze the bonding in these complexes and to assign the photoelectron spectra. Ligand-metal interaction is found to be predominantly ionic in character, in contrast to the strong d and f covalency of related divalent transition-metal and tetravalent f-element bis(annulene) compounds. Some of the 4f ionizations are clearly identified for  $\text{Sm}(\text{C}_5\text{Me}_5)_2$  and  $\text{Yb}(\text{C}_5\text{Me}_5)_2$ , and their ionization energy may be inferred for  $\text{Eu}(\text{C}_5\text{Me}_5)_2$ . Increases in the intensity of the f bands relative to the cyclopentadienyl  $\pi$ -ionizations range from four- to ninefold.

## 1. Introduction

A variety of first-row transition metals form bis(cyclopentadienyl) sandwich compounds. It is a generally held view, however, that for f elements the appropriate ring for bis(carbocycle) sandwich complexes consists of eight members to fit the larger atomic radius of the metal.<sup>1,2</sup> Until recently, bis(cyclopentadienyl)lanthanide compounds were only known with additional coordination sites at the metal occupied either by adduct molecules (e.g. ref 3) or by oligomerization (e.g. ref 4), with the two rings tilted accordingly.

Now, successful preparations of monomeric homoleptic bis(pentamethylcyclopentadienyl) complexes  $\text{Ln}(\text{C}_5\text{Me}_5)_2$  have been achieved for those lanthanides that commonly show divalent chemistry, namely, Sm,<sup>5</sup> Eu,<sup>6</sup> and Yb.<sup>6</sup> Two structure determinations have been performed so far, also revealing geometries with tilted rings. For  $\text{Yb}(\text{C}_5\text{Me}_5)_2$ , a ring centroid-Ln-ring centroid angle of 156° has been determined from gas-phase electron diffraction (ED) measurements.<sup>7</sup> Crystal X-ray data of the samarium complex<sup>5</sup> show an angle of 140° that is remarkably close to that found for the solvated THF analogue.<sup>5</sup> The origin of these structural distortions is of sufficient interest to attempt theoretical calculations on both parallel and bent geometries in a search for a possible orbital explanation.

Bonding in transition-metal cyclopentadienyl complexes is primarily between the  $e_1(\pi)$  orbitals of the ring and the metal d orbitals, though ring  $a(\pi)$  orbitals and metal s and p orbitals may also participate.<sup>8</sup> Molecular orbital (MO) calculations have shown for bis([8]annulene) compounds of uranium and thorium that ring-metal bonding is quite

covalent with substantial contributions from metal f orbitals.<sup>9,10</sup> Recently, the bonding in the analogous cerium compound has been interpreted as being quite similar, again on the combined analysis of He I and He II photoelectron (PE) spectra and MO calculations.<sup>10,11</sup>

In the same spirit, we would like to discuss here the electronic structure of bis(cyclopentadienyl)lanthanide complexes and compare it with that of transition metal as well as actinide sandwich compounds. We will present PE spectra of  $\text{Ln}(\text{C}_5\text{Me}_5)_2$  (Ln = Sm, Eu, Yb), and molecular orbital calculations on the corresponding model systems  $\text{Ln}(\text{C}_5\text{H}_5)_2$  (Ln = Eu, Yb). Part of this work has already been the subject of a preliminary communication.<sup>12</sup> Here we carry out further analysis of the PE spectra in order to obtain values for the relative intensities of the f and cyclopentadienyl  $\pi$ -ionizations when subject to He I and He II radiation.

## 2. Experimental and Computational Details

The compounds  $\text{Ln}(\text{C}_5\text{Me}_5)_2$ , where Ln = Sm, Eu, and Yb, were prepared in Berkeley.<sup>12</sup>

He I and He II photoelectron spectra were obtained by using a PES Laboratories photoelectron spectrometer interfaced with a Research Machines 380Z microprocessor for data collection. Spectra were collected by repeated scans of ca. 30 s in order to minimize relative intensity changes of the bands; though the compounds tended to degrade the instrumental resolution, there was no apparent drift during data collection. The spectra were calibrated by simultaneous measurement of the PE spectra of He, Xe, and N<sub>2</sub>. In the spectra given in Figure 1 of  $\text{Eu}(\text{C}_5\text{Me}_5)_2$ , the points represent the raw experimental data and the solid line represents a least-squares fit to these points. The spectra of the low-energy region bands are shown in Figures 2-4.

Relative intensities of the low-energy bands were determined by using a curve-fitting program. The relative intensities and separation of the f-band components were

(1) Schumann, H. *Angew. Chem.* 1984, 96, 475.(2) Marks, T. J.; Ernst, R. D. In *Comprehensive Organometallic Chemistry*; Wilkinson, G., Stone, F. G. A., Abel, E. W., Eds.; Pergamon Press: Oxford, 1982; Vol. 9, p 1209.(3) Tilley, T. D.; Andersen, R. A.; Spencer, B.; Ruben, H.; Zalkin, A.; Templeton, D. H. *Inorg. Chem.* 1980, 19, 2999. T. D. Tilley, Andersen, R. A.; Spencer, B.; Zalkin, A. *Inorg. Chem.* 1982, 21, 2647.(4) Zinnen, H. A.; Pluth, J. J.; Evans, W. J. *J. Chem. Soc., Chem. Commun.* 1980, 810.(5) Evans, W. J.; Hughes, L. A.; Hanusa, T. P. *J. Am. Chem. Soc.* 1984, 106, 4270.(6) Boncella, J. M.; Burns, C. J.; Andersen, R. A. *Inorg. Chem.*, in press.(7) Andersen, R. A.; Boncella, J. M.; Burns, C. J.; Blom, R.; Haaland, A.; Volden, H. V. *J. Organomet. Chem.* 1986, 312, C49.(8) Lauher, J. W.; Hoffmann, R. *J. Am. Chem. Soc.* 1976, 98, 1729.(9) Rösch, N.; Streitwieser, A., Jr. *J. Am. Chem. Soc.* 1983, 105, 7237.(10) Rösch, N. *Inorg. Chim. Acta* 1984, 94, 297.(11) Streitwieser, A., Jr.; Kingsley, S. A.; Rigsbee, J. T.; Fragala, I. L.; Ciliberto, E.; Rösch, N. *J. Am. Chem. Soc.* 1985, 107, 7237.(12) Andersen, R. A.; Boncella, J. M.; Burns, C. J.; Green, J. C.; Hohl, D.; Rösch, N. *J. Chem. Soc., Chem. Commun.* 1986, 405.

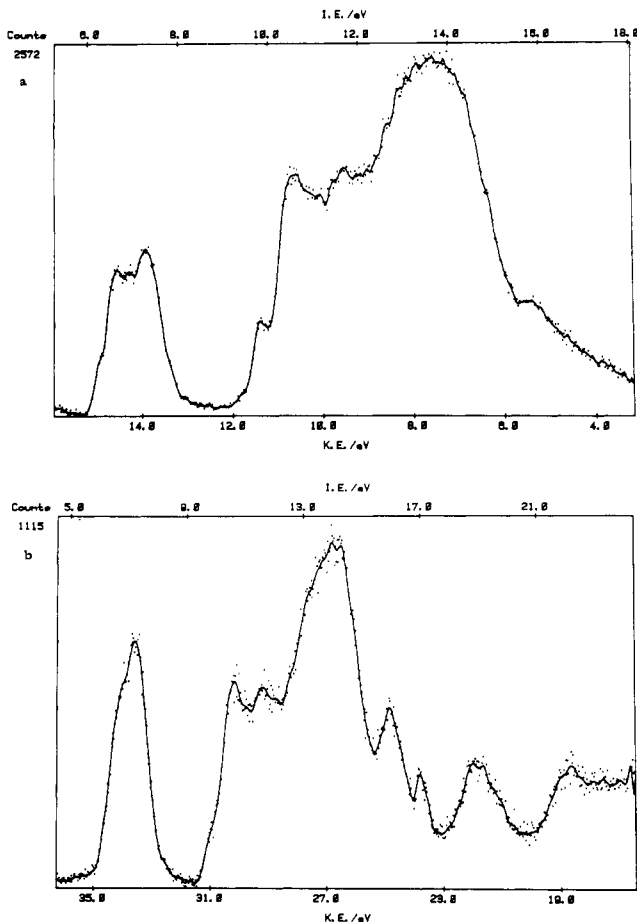


Figure 1. Full range (a) He I spectrum and (b) He II spectrum of  $\text{Eu}(\text{C}_5\text{Me}_5)_2$ .

fixed according to the predictions of Cox's rules<sup>13</sup> and literature values for the separation of the ion states for  $\text{Ln}^{3+}$  ions.<sup>14</sup> This approach that amounts to an essentially atomic interpretation of the f bands seems fully justified in the light of the calculations to be discussed below (see sections 3.1 and 3.2). Three or four asymmetric Gaussians were used to fit the cyclopentadienyl  $e_1$  band, in order to estimate the remaining band area. The fits were restricted by the same vertical ionization energies for each Gaussian being used in both He I and He II spectra, the relative intensities of the various f states being determined according to Cox's rules and their separations from established values for  $\text{Ln}^{3+}$  from the literature. In the cases of the f states symmetric Gaussians were used and the same width was used for each state. As a consequence, given an initial choice of band width and placing for the most evident f state, the residual area of the low-energy bands was determined. The placing and relative magnitude of the bands used to fit this residual area has no interpretative significance beyond this. The resultant fits are shown in Figures 2-4. In all cases the root-mean-square deviation was less than 2.2%. The areas found were divided by the kinetic energies of the photoelectrons to obtain values corrected for the discrimination of the analyzer against slow electrons.

The calculations were performed by using the SCF- $X\alpha$ -scattered-wave (SW) method (for a review see ref 15). Although this method has been used in numerous inves-

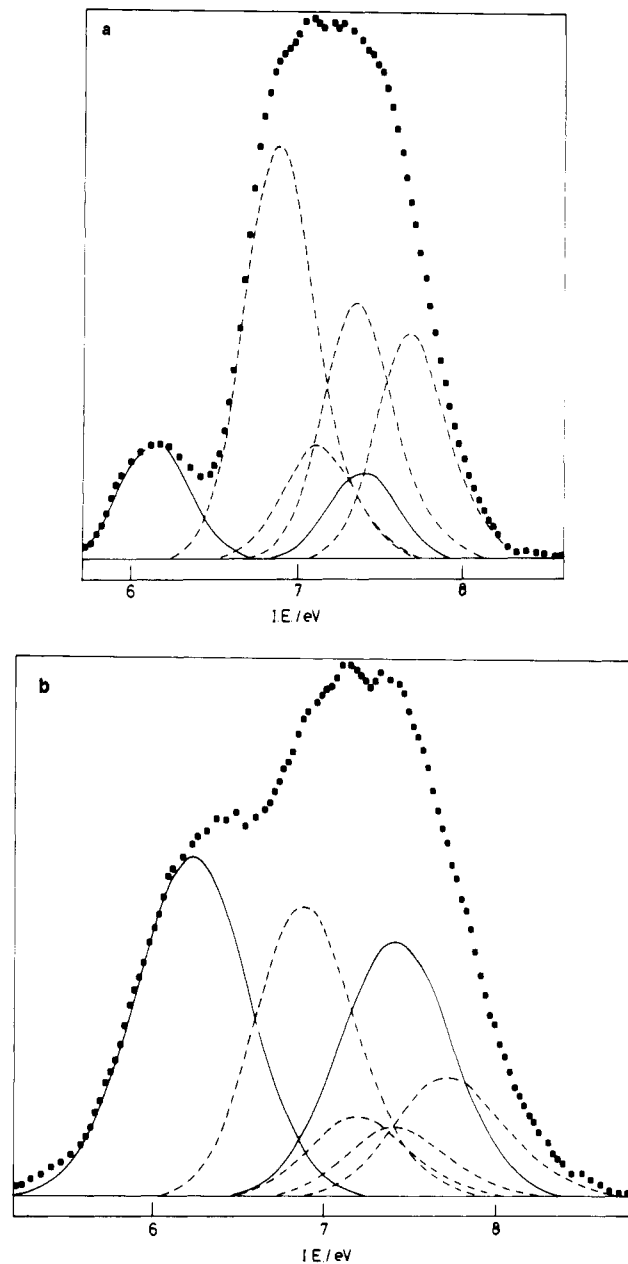


Figure 2. Fit of bands to the low-energy region of the (a) He I and (b) He II spectrum of  $\text{Yb}(\text{C}_5\text{Me}_5)_2$ . The solid lines delineate the f bands and the dashed lines the cyclopentadienyl bands.

tigations of a wide variety of molecules and clusters, applications to lanthanide complexes are rather limited to date. Apart from the calculation of cerocene<sup>9,11</sup> only fluoro and oxo complexes have been examined.<sup>16,17</sup> In a rather extensive investigation, PE spectra and electronic structure of lanthanide trihalides have been studied by using the more accurate DVM- $X\alpha$  method.<sup>18</sup> It was found that the inclusion of relativistic effects leads to improved agreement with experiment. We have therefore used a quasi-relativistic version of the  $X\alpha$ -SW method<sup>19,20</sup> that has proven well-suited for large molecules containing heavy elements.<sup>9,19</sup> Previous  $X\alpha$ -SW calculations of cyclo-

(16) Weber, J.; Berthou, H.; Jørgensen, C. K. *Chem. Phys. Lett.* 1977; 45, 1; *Chem. Phys.* 1977, 26, 69.

(17) Case, D. A.; Lopez, J. P. *J. Chem. Phys.* 1984, 80, 3270.

(18) Ruscic, B.; Goodman, G. L.; Berkowitz, J. *J. Chem. Phys.* 1983, 78, 5443.

(19) Thornton, G.; Rösch, N.; Edelstein, N. *Inorg. Chem.* 1980, 19, 1304.

(20) Heera, V.; Seifert, G.; Ziesche, P. *J. Phys. B: At. Mol. Phys.* 1984, 17, 519.

(13) Cox, P. A. *Struct. Bonding (Berlin)* 1975, 24, 59.

(14) Carnall, W. T.; Fields, P. R.; Rajnak, K. *J. Chem. Phys.* 1968, 49, 4412, 4424.

(15) Rösch, N. In *Electrons in Finite and Infinite Structures*; Pharisseau, P., Scheire, L., Eds.; Plenum: New York, 1977; p 1.

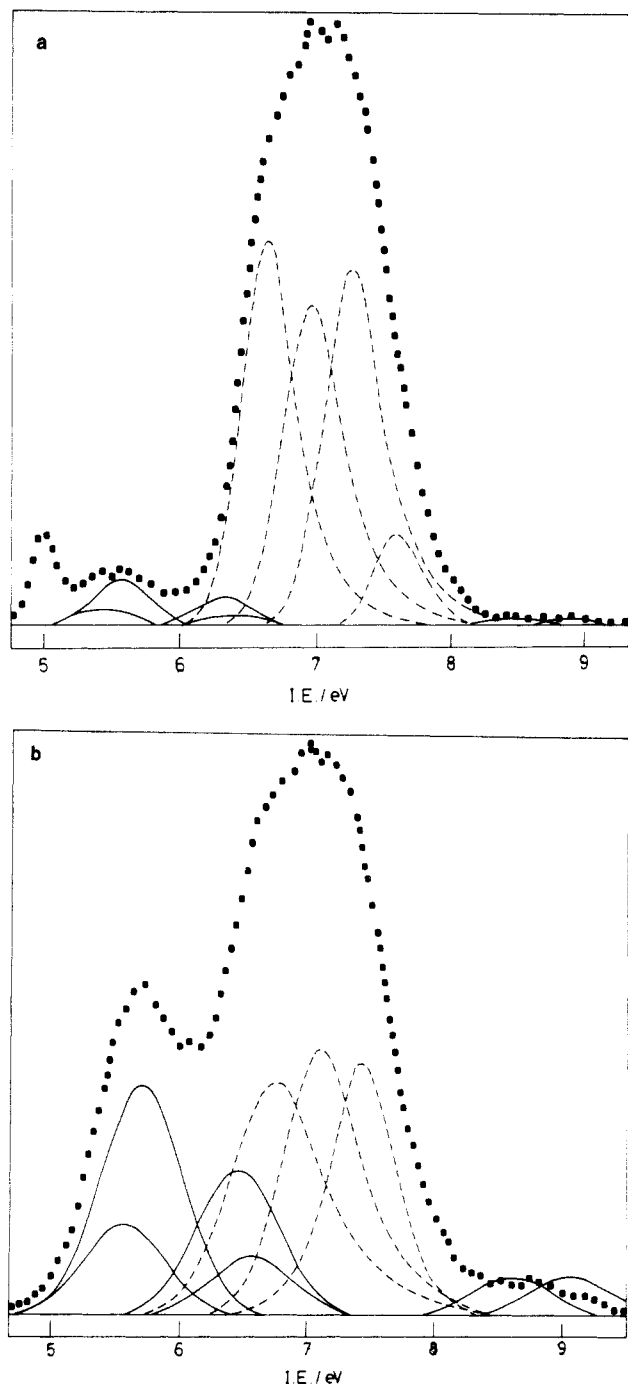


**Figure 3.** Fit of bands to the low-energy region of the (a) He I and (b) He II spectrum of  $\text{Sm}(\text{C}_5\text{Me}_5)_2$ . The solid lines represent the f bands and the dashed lines the cyclopentadienyl bands.

pentadienyl sandwich compounds  $\text{M}(\text{C}_5\text{H}_5)_2$  include transition metals ( $\text{M} = \text{Mn},^{21} \text{Fe},^{22} \text{Co},^{23} \text{Ni}^{24}$ ) as well as main-group elements ( $\text{M} = \text{Be}, \text{Sn}^{25}$ ). Recently a muffin-tin free LCGTO- $X\alpha$  geometry study of ferrocene has been reported.<sup>26</sup>

To reduce computational effort, the model systems  $\text{Eu}(\text{C}_5\text{H}_5)_2$  and  $\text{Yb}(\text{C}_5\text{H}_5)_2$  have been calculated. The

(21) Weber, J.; Goursot, A.; Penigault, E. *J. Mol. Struct.* **1980**, *60*, 397.

(22) Rösch, N.; Johnson, K. H. *Chem. Phys. Lett.* **1974**, *24*, 179.

(23) Goursot, A.; Penigault, E.; Weber, J. *Nouv. J. Chim.* **1979**, *3*, 675.

(24) Weber, J.; Goursot, A.; Penigault, E.; Ammeter, J. H.; Bachmann, J. *J. Am. Chem. Soc.* **1982**, *104*, 1491.

(25) Baxter, S. G.; Cowley, A. H.; Lasch, J. G.; Lattman, M.; Sharum, W. P.; Stewart, C. A. *J. Am. Chem. Soc.* **1982**, *104*, 4064. Lattman, M.; Cowley, A. H. *Inorg. Chem.* **1984**, *23*, 241.

(26) Rösch, N.; Jörg, H. *J. Chem. Phys.* **1986**, *84*, 5967.

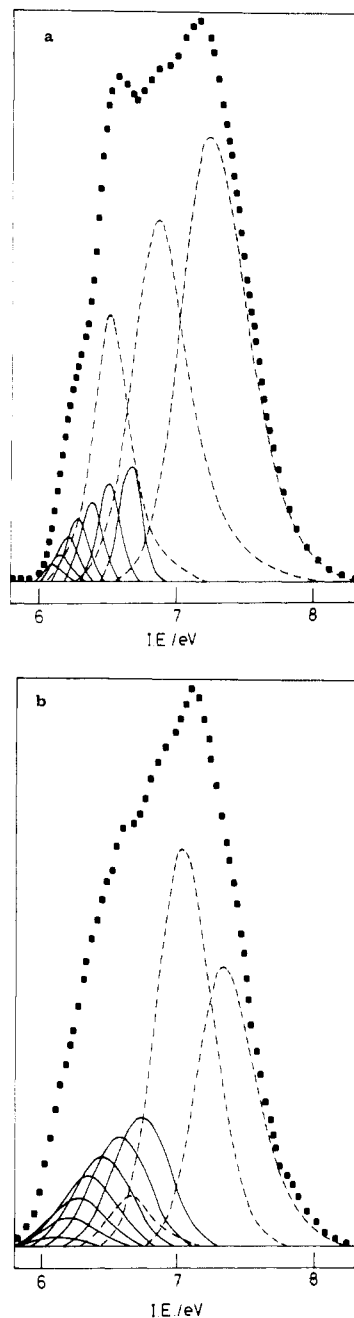


**Figure 4.** Fit of bands to the low-energy region (a) He I and (b) He II spectrum of  $\text{Eu}(\text{C}_5\text{Me}_5)_2$ . The solid lines delineate the f bands and the dashed lines the cyclopentadienyl bands.

ring-metal bonding in these molecules should be rather similar to that in the permethylated analogues, where the methyl groups provide effective steric shielding. However, these substituents will reduce the ionization energies (IE) as was shown in a detailed study on the metallocenes of the transition elements.<sup>27</sup>

No gas-phase structure was available when these calculations were started. Therefore the first calculations were performed with a hypothetical geometry. The two rings were chosen planar and parallel in a staggered configuration (symmetry group  $D_{5d}$ ). The carbon-metal distance was deduced by assigning effective ionic radii to both the metal and the pentamethylcyclopentadienyl ring.<sup>28</sup> From various f-block metal complexes one derives a fairly

(27) Cauletti, C.; Green, J. C.; Kelly, M. R.; Powell, P. van Tilborg, J.; Robbins, J.; Smart, J. *J. Electron Spectrosc. Relat. Phenom.* **1980**, *19*, 327.

(28) Raymond, K. N.; Eigenbrot, C. W. *Acc. Chem. Res.* **1980**, *13*, 276.

**Table I. Bond Lengths,<sup>a</sup> Bond Angles,<sup>a</sup> and Muffin-Tin Sphere Radii<sup>c</sup> Used in the Calculations**

	Yb(C <sub>5</sub> H <sub>5</sub> ) <sub>2</sub>		Eu(C <sub>5</sub> H <sub>5</sub> ) <sub>2</sub>
	C <sub>2v</sub>	D <sub>5d</sub>	D <sub>5d</sub>
d(Ln-C)	2.610 <sup>b</sup>	2.620	2.770
d(C-C)	1.410	1.410	1.410
d(C-H)	1.100	1.100	1.100
∠Cp-Ln-Cp <sup>c</sup>	156	180	180
r(M) <sup>d</sup>	1.565	1.565	1.700
r(C)	0.881	0.881	0.881
r(H)	0.494	0.494	0.494

<sup>a</sup>All lengths in Å; all angles in deg. <sup>b</sup>From gas-phase electron diffraction analysis of Yb(C<sub>5</sub>Me<sub>5</sub>)<sub>2</sub>,<sup>7</sup> see section 2. <sup>c</sup>Cp(centroid)-Ln-Cp(centroid) angle. <sup>d</sup>Metal sphere radius determined by Norman's procedure<sup>30</sup> using a scaling factor of 0.90.

constant radius of 1.64 ± 0.04 Å for the cyclopentadienyl ring (perpendicular to the ring).<sup>3,28</sup> Since, in the present case, there are no further ligands increasing the size of the coordination sphere, the smallest value, compatible with this range, was chosen. Taking the ionic radius of Yb<sup>2+</sup> for sixfold coordination,<sup>29</sup> one obtains a Yb-C distance of 2.62 Å, very close to the reported ED value of 2.61 Å. A Eu-C distance of 2.77 Å was deduced in the same manner. The C<sub>5</sub>H<sub>5</sub><sup>-</sup> ring geometry was chosen to mimic C<sub>5</sub>Me<sub>5</sub><sup>-</sup> with a C-C bond distance of 1.41 Å and a standard C-H bond length of 1.10 Å. For Yb(C<sub>5</sub>H<sub>5</sub>)<sub>2</sub>, a calculation consistent with the available ED structure data<sup>7</sup> was also performed. Pertinent structural data used in the various calculations are collected in Table I.

As in previous calculations,<sup>22,23</sup> an overlapping sphere parameterization was used for the rings, to obtain a more realistic description of the ring π-system and the ring-metal interaction. The geometry-determined touching sphere radii of carbon and hydrogen were increased by 25%.<sup>22</sup> If the metal sphere were then chosen to touch the carbon sphere, unusually large metal radii would result, e.g. for Yb 1.74 Å. These large spheres for Eu and Yb are virtually identical with those enclosing that portion of the superimposed free atom charge densities required to balance the nuclear charge.<sup>30</sup> In the standard parameter set we have therefore reduced the metal radius to 90% of the touching sphere value following Norman's procedure.<sup>30</sup> Calculations with touching metal and carbon spheres have also been performed. They showed no significant differences except for somewhat larger localizations in the metal sphere. Essential muffin-tin radii of the various model systems are displayed in Table I.

The maximum *L* values in the partial wave expansions included in the calculations were *L* = 3 in the metal sphere, *L* = 1 for carbon, *L* = 0 for hydrogen, and *L* = 5 in the extramolecular region.

The exchange parameters  $\alpha$  for carbon and hydrogen were taken as in previous calculations.<sup>22,23</sup> The parameters  $\alpha$  for the metals were taken from the tables provided by Schwarz.<sup>31</sup> A weighted average of the atomic values was employed in the extra molecular region. The core charge densities, C ([He]), Eu, and Yb ([Kr]), were kept fixed as obtained from atomic X $\alpha$  calculations (of relativistic type for the lanthanides). All other electrons were considered fully in the iterations toward self-consistency, spin-orbit interaction being neglected. Spin polarization effects in the Eu complex were taken into account in a separate calculation as discussed in section 3.2. Slater's transition

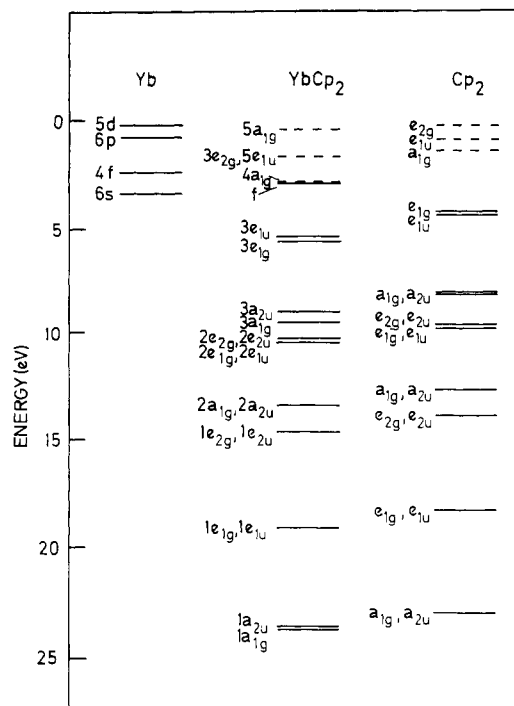


**Figure 5.** X $\alpha$ -SW valence orbital energies of Yb(C<sub>5</sub>H<sub>5</sub>)<sub>2</sub> for D<sub>5d</sub> geometry. Also shown for comparison are the orbital energies of the empty cluster (C<sub>5</sub>H<sub>5</sub>)<sub>2</sub> and the Yb atom. Occupied orbitals are indicated by solid lines and empty ones by dashed lines.

state procedure was used to compute the ionization energies.<sup>32</sup>

To evaluate the metal-ring interaction, a cluster of two neutral cyclopentadienyl rings was also calculated employing the same muffin-tin geometry as that for the Yb complex with an "empty" sphere present in place of the metal atom.<sup>9,15</sup> The configuration used for the SCF-X $\alpha$  calculation of this cluster was e<sub>1g</sub><sup>4</sup>e<sub>2u</sub><sup>2</sup>. The orbital energy spectrum and the orbital localizations of this artificial cluster provide a better reference for a comparison of the results of the actual complex than the corresponding quantities of a single cyclopentadienyl ring, since the errors due to the muffin-tin form of the electronic potential should be similar for both sandwich systems.

### 3. Results and Discussion

#### 3.1. Bis(pentamethylcyclopentadienyl)ytterbium.

**3.1.1. The Molecular Orbitals of the Sandwich Compound in D<sub>5d</sub> Symmetry.** The idealized model with parallel rings is used as a reference in our discussion of the electronic structure of the bis(pentamethylcyclopentadienyl)lanthanide complexes. The high symmetry facilitates both the calculations and the analysis of the results as well as comparison with previous investigations of d-block metallocenes.<sup>22,23</sup> The staggered D<sub>5d</sub> configuration was chosen for convenience.<sup>22</sup> It has been shown for ferrocene that both the eclipsed (D<sub>5h</sub>) and the staggered configuration yield essentially the same results.<sup>22</sup> In the present system, the differences are expected to be even smaller, due to the more ionic character of the ring-metal bond.

The MO spectrum of Yb(C<sub>5</sub>H<sub>5</sub>)<sub>2</sub> and the corresponding charge distribution over the various muffin-tin regions are shown in Table II. In Figure 5 we compare the X $\alpha$  orbital energies of the complex with the corresponding level

(29) Shannon, R. D. *Acta Crystallogr., Sect. A: Cryst. Phys., Diffraction, Gen. Crystallogr.* 1976 A32, 751.

(30) Norman, J. G. *Mol. Phys.* 1976, 31, 1191.

(31) Schwarz, K. *Phys. Rev.* 1972, 85, 2466; *Theor. Chim. Acta* 1974, 34, 225.

(32) Slater, J. C. *The Self-Consistent Field for Molecules and Solids*, McGraw-Hill: New York, 1974.

Table II.  $X\alpha$ -SW Ground-State Orbital Energies (eV) and Charge Distribution<sup>a</sup> for  $YbCp_2$ 

orbital <sup>b</sup>	energy	Yb				C	H	intersphere	outersphere
		s	p	d	f				
5e <sub>1u</sub>	-1.63		0.008		0.036	0.071	0.003	0.509	0.374
3e <sub>2g</sub>	-1.68			0.241		0.103	0.001	0.522	0.133
4a <sub>1g</sub>	-2.84	0.074		0.098		0.047	0.004	0.624	0.155
4e <sub>1u</sub> <sup>c</sup>	-2.85		0.004		0.940	0.006		0.042	0.008
4a <sub>2u</sub>	-2.88				0.994			0.006	
4e <sub>2u</sub>	-2.90				0.993			0.007	
3e <sub>2u</sub>	-2.92				0.984	0.006		0.010	
3e <sub>1u</sub>	-5.43		0.027		0.028	0.587		0.309	0.048
3e <sub>1g</sub>	-5.68			0.094		0.578		0.289	0.038
3a <sub>2u</sub>	-8.90		0.041		0.001	0.630		0.283	0.046
3a <sub>1g</sub>	-9.41	0.057		0.020		0.583		0.299	0.041
2e <sub>2u</sub>	-10.20					0.651	0.172	0.145	0.031
2e <sub>2g</sub>	-10.21					0.652	0.171	0.153	0.024
2e <sub>1g</sub>	-10.33			0.001		0.608	0.207	0.152	0.032
2e <sub>1u</sub>	-10.33				0.001	0.607	0.205	0.150	0.037
2a <sub>2u</sub>	-13.27				0.002	0.556	0.200	0.204	0.038
2a <sub>1g</sub>	-13.30			0.003		0.552	0.199	0.211	0.036
1e <sub>2u</sub>	-14.51				0.001	0.782	0.079	0.119	0.019
1e <sub>2g</sub>	-14.52			0.001		0.779	0.080	0.124	0.016
1e <sub>1u</sub>	-18.94		0.003		0.003	0.849	0.039	0.094	0.012
1e <sub>1g</sub>	-18.97			0.006		0.847	0.039	0.096	0.012
1a <sub>2u</sub>	-23.52		0.020		0.002	0.915	0.007	0.051	0.006
1a <sub>1g</sub>	-23.67	0.007		0.007		0.918	0.007	0.055	0.005

<sup>a</sup>Fractions of orbital localization per type of muffin-tin region. For the metal sphere the contributions of the various partial waves are shown. <sup>b</sup>The corelike orbitals Yb 5s and 5p, although included in the SCF process, are not displayed. <sup>c</sup>Highest occupied orbital.

spectrum of the  $(C_5H_5)_2$  "dimer". Also shown are the spin-orbit averaged levels of the Yb atom from a relativistic  $X\alpha$  calculation.

The low-lying levels 1a<sub>1g</sub> to 2e<sub>2u</sub> describe the  $\sigma$  bonds within the cyclopentadienyl ligands. With respect to the  $(C_5H_5)_2$  dimer, all these levels undergo a uniform downward shift of 0.7 eV.

The next six MOs (3a<sub>1g</sub>, 3a<sub>2u</sub>, 3e<sub>1g</sub>, and 3e<sub>1u</sub>) hold the ring  $\pi$ -electrons and may contribute to a covalent ring-metal interaction. This can be monitored by their localization within the metal sphere (see Table II) and from the shift compared with that of the  $(C_5H_5)_2$  dimer. Both quantities are found to be nicely correlated. The values for the shift are -1.25, -0.88, -1.41, and -0.99 eV (in the order quoted above) and the corresponding charge fractions are 0.077, 0.042, 0.094, and 0.055. This interaction-induced ranking of the ring  $\pi$ -orbitals is the same as that found in ferrocene.<sup>22</sup> However, the amount of metal contribution to these orbitals—and consequently the covalent ligand-metal bonding—is much larger in the d-block metallocene, namely, 0.16, 0.09, 0.30, and 0.09. The differences between the two sandwich complexes become even more pronounced when one takes into account that the radius of the Yb sphere is 10% larger than that of the Fe sphere.<sup>22</sup>

The next seven orbitals in the level spectrum (3e<sub>2u</sub> to 4e<sub>1u</sub>) are strongly localized within the Yb sphere; they hold the filled f shell of Yb. These levels are ordered as expected from formal overlap considerations. The 4e<sub>1u</sub> level lies highest as the antibonding partner of the ring 3e<sub>1u</sub> orbital. The 3e<sub>2u</sub> level, composed mainly of the  $f_{xz}^2$  and  $f_{yz}^2$  orbitals of Yb would be the one to carry the back-bonding; it has the lowest energy in the manifold. However, the metal sphere localization deviates noticeably from 1.00 only in the top 4e<sub>1u</sub> orbitals. The splitting of the f orbitals in the ligand field of the cyclopentadienyl rings is only 0.07 eV. This is substantially smaller than the spin-orbit splitting of 1.33 eV estimated from perturbation theory. Therefore, it seems more appropriate to derive, from the present level spectrum, only a center of gravity of the Yb 4f manifold (at -2.89 eV).

The remaining orbitals, 4a<sub>1g</sub>, 3e<sub>2g</sub>, and 5e<sub>1u</sub> are empty in  $Yb(C_5H_5)_2$ . These orbitals are significantly delocalized over

Table III. Partial Wave Analysis of the Charge Localized in the Metal Sphere of  $Ln(C_5H_5)_2$  ( $Ln = Yb, Eu$ ) and in the Empty Sphere of  $(C_5H_5)_2$ 

	Yb( $C_5H_5$ ) <sub>2</sub>		Eu( $C_5H_5$ ) <sub>2</sub>		$(C_5H_5)_2^a$
	f <sup>14</sup>	f <sup>0b</sup>	f <sup>7</sup>	f <sup>0b</sup>	
s	0.127	0.127	0.095	0.095	0.091
p	0.259	0.245	0.430	0.417	0.177
d	0.473	0.473	0.481	0.481	0.070
f	13.798	0.143	6.935	0.149	0.039
total	14.657	0.988	7.941	1.130	0.377

<sup>a</sup>The same muffin-tin geometry has been used as in the ytterbium complex. <sup>b</sup>Without the contribution from the Ln 4f orbitals. Only ligand-derived molecular orbitals are included.

the whole complex, including the intersphere and outersphere region (see Table II). They, therefore, cannot be assigned to specific atomic orbitals. Two of the levels, 4a<sub>1g</sub> (LUMO) and 3e<sub>2g</sub>, show definite contributions from Yb 5d orbitals, an ordering similar to that found for the d orbitals of the transition-metal metallocenes,<sup>8,22</sup> i.e. a<sub>1g</sub> and e<sub>2g</sub> below e<sub>1g</sub>. The missing e<sub>1g</sub> level lies too high to be detected in the present calculation.

From the preceding analysis of the MOs, it has become quite evident that covalent contributions to metal-ring bonding in  $Yb(C_5H_5)_2$  are rather small. Clear indications for ionic interaction are provided by the weak ligand field splitting of the 4f orbitals and by their strong localization, as well as by the small charge localization of the ligand-derived orbitals inside the metal sphere.

In order to appreciate the size of these charge localizations, it is instructive to compare the metal populations of the key orbitals for ring-metal bonding in  $Yb(C_5H_5)_2$  to the corresponding orbitals of  $Ce(C_5H_5)_2$ .<sup>10</sup> In  $Yb(C_5H_5)_2$ , the orbitals 3e<sub>1g</sub> and 3e<sub>1u</sub> have metal populations of 0.094 and 0.055, respectively (see Table II). The essential orbitals of  $Ce(C_5H_5)_2$  are e<sub>2g</sub> and e<sub>2u</sub> with localization values of 0.206 and 0.330.<sup>10</sup> Although this comparison is somewhat hampered by the differing sphere radii in the two calculations, the large localization differences certainly reflect the disparate character of the ring-metal bonding.

To elaborate on this point, we have collected in Table III the total partial wave populations in the metal sphere

Table IV. Vertical Ionization Energies (eV) for Ln(C<sub>5</sub>Me<sub>5</sub>)<sub>2</sub> (Ln = Sm, Eu, and Yb)

Sm	Eu	Yb
5.37 A <sub>1</sub>	6.29 A <sub>1</sub>	6.11 A <sub>1</sub>
5.57 A <sub>2</sub>		
7.05 A <sub>3</sub>	6.61 A <sub>2</sub>	7.11 A <sub>2</sub>
	7.25 A <sub>3</sub>	
9.9 B <sub>1</sub>	9.8 B <sub>1</sub>	10.1 B <sub>1</sub>
10.7 B <sub>2</sub>	10.5 B <sub>2</sub>	10.9 B <sub>2</sub>
11.4 B <sub>3</sub>	11.6 B <sub>3</sub>	12.0 B <sub>3</sub>
13.4 B <sub>4</sub>	13.4 B <sub>4</sub>	13.8 B <sub>4</sub>
15.9 B <sub>5</sub>	15.9 B <sub>5</sub>	16.1 B <sub>5</sub>
18.9 C <sub>1</sub>	18.9 C <sub>1</sub>	19.0 C <sub>1</sub>
22.4 C <sub>2</sub>	22.2 C <sub>2</sub>	22.0 C <sub>2</sub>

for the valence electrons of Yb(C<sub>5</sub>H<sub>5</sub>)<sub>2</sub>. The contributions from the ligand-derived orbitals are shown separately in order to isolate the covalency effects. In cerocene, the main contributions to covalent ring-metal bonding have been shown to originate from metal d and f orbitals.<sup>9,10</sup> Their corresponding total partial wave populations were found to be 1.617 and 1.619, respectively.<sup>10</sup> A comparison with the d and f occupations in Yb(C<sub>5</sub>H<sub>5</sub>)<sub>2</sub>, 0.473 and 0.143, corroborates the conclusion that the bonding in the present cyclopentadienyl sandwich compounds is mainly of ionic character.

A rather striking feature of the level spectrum of Yb(C<sub>5</sub>H<sub>5</sub>)<sub>2</sub> is the almost vanishing HOMO-LUMO gap, 4e<sub>1u</sub> to 4a<sub>1g</sub> (see Table II). It is well-known that X $\alpha$  orbital energies cannot be compared directly with experimental ionization energies.<sup>15,32</sup> By the same token, orbital energy differences may not be interpreted as excitation energies rather one has to employ Slater's transition-state procedure,<sup>32</sup> where half an electron is moved, either between orbitals whose excitation energy is to be calculated or from the system altogether for an ionization process. The energy relaxation calculated in the latter case reflects the change of the orbital due to ionization and the removal of a self-energy contribution contained in the ground-state one-electron energy.<sup>15,32</sup> For excitations, the self-energy difference of the orbitals in question will be the more important correction to the ground-state orbital energy difference. From these considerations, it is clear that one has to expect especially large transition-state relaxation effects for the spatially very compact 4f orbitals of the lanthanides. This is also borne out in the various transition-state calculations (see section 3.3). The HOMO-LUMO energy difference,  $E(4a_{1g}) - E(4e_{1u})$  rises from 0.01 eV in the ground state to 1.66 eV in the appropriate transition state, 4e<sub>1u</sub><sup>3.5</sup>4a<sub>1g</sub><sup>0.5</sup>. The calculated excitation energy corresponds to an absorption around 750 nm, somewhat too long a wavelength to account for the green<sup>33</sup> or red<sup>34</sup> color reported for polymeric Yb(C<sub>5</sub>H<sub>5</sub>)<sub>2</sub>. More intense than the HOMO-LUMO transition may be the ligand to metal charge-transfer excitation 3e<sub>1u</sub> to 4a<sub>1g</sub>. The transition-state procedure yields an excitation energy of 2.7 eV corresponding to an absorption around 460 nm. The f to d transition 4e<sub>2u</sub> to 3e<sub>2g</sub> also leads to an absorption wavelength (390 nm) close to the visible part of the spectrum. As spin-orbit effects have been neglected in these estimates, an exact agreement with experiment is not expected.

**3.1.2. The Structure with Tilted Rings.** Bis(ring) sandwich compounds frequently exhibit a structure with tilted rings due to the interaction of metal d orbitals with

those of further ligands<sup>8</sup> or induced by a metal lone pair as in stannocene.<sup>25</sup> In the case of Yb(C<sub>5</sub>Me<sub>5</sub>)<sub>2</sub> neither one of the explanations can be used to rationalize the observed structure. A calculation on the tilted ring structure was carried out, first as this is the established experimental geometry and second to establish whether a calculation would indicate why this was the case.

The X $\alpha$ -SW calculation on the model structure with parallel cyclopentadienyl rings has confirmed the expected ionic bonding with highly localized Yb 4f electrons and negligible ring metal donation. Therefore the shape of the occupied orbitals should not change much on going over to the experimental structure with tilted rings.

A calculation in C<sub>2v</sub> symmetry with a structure based on the ED data<sup>7</sup> has been performed. All parameters were left unchanged except for the ring-Yb-ring angle, the (tangent) outersphere and a slight adjustment of the Yb-C distance (see Table I). Just as anticipated, no significant differences from the D<sub>5d</sub> results were observed in the molecular orbital spectrum and the orbital charge distributions (except in the LUMO, see below). Therefore we refrain from displaying the C<sub>2v</sub> results in a manner comparable to that in Table II. The C<sub>2v</sub> orbital spectrum may easily be constructed from that of D<sub>5d</sub> symmetry if one uses the correlations a<sub>1g</sub>  $\rightarrow$  a<sub>1</sub>, a<sub>2u</sub>  $\rightarrow$  b<sub>2</sub>, e<sub>1g</sub>  $\rightarrow$  a<sub>2</sub> + b<sub>2</sub>, e<sub>1u</sub>  $\rightarrow$  a<sub>1</sub> + b<sub>1</sub>, e<sub>2g</sub>  $\rightarrow$  a<sub>1</sub> + b<sub>1</sub>, and e<sub>2u</sub>  $\rightarrow$  a<sub>2</sub> + b<sub>2</sub>. (Note the exception, 4e<sub>2u</sub>(f<sub>x<sup>3</sup>-3xy<sup>2</sup>, f<sub>y<sup>3</sup>-3yx<sup>2</sup></sub>)  $\rightarrow$  a<sub>1</sub> + b<sub>1</sub>!) These correlations are based on a change in coordinate system x  $\rightarrow$  y, y  $\rightarrow$  z, and z  $\rightarrow$  x, when going from D<sub>5d</sub> to C<sub>2v</sub>. Level shifts or splittings average to 0.1 eV but are never larger than 0.25 eV, this value occurring for the center of gravity of the highly localized f orbitals. The comparison of the orbital charge distributions was based on appropriate sums over the descendants from a D<sub>5d</sub> level pair. It would certainly not be meaningful to interpret the observed small differences.</sub>

Within a MO model such as the one used here, no explanation can be given for the observed bent structure of Yb(C<sub>5</sub>Me<sub>5</sub>)<sub>2</sub>. Because of its ionic character, one would expect a structure with parallel rings, and bending should be feasible at practically no energetic expense. The same conclusions have been reached by Ortiz and Hoffmann in their recent extended Hückel MO study on cyclopentadienyllanthanide hydrides.<sup>35</sup> For a rationalization of the tilted ring structure, one may have to resort to electrostatic considerations within the polarizable ion model.<sup>36,37</sup> This model has proven useful for understanding structural trends in metal di- and trihalides. Correct predictions have been obtained for all lanthanide di- and trihalide structures that had been characterized experimentally at that time.<sup>38</sup> This model attributes bent structures of metal dihalides to increased attractive interaction between the metal and halogen ions of the types charge-induced dipole, dipole-charge, and dipole-dipole;<sup>39</sup> these outweigh the increased interhalogen charge-charge and induced dipole-dipole repulsion. It seems quite plausible that an argument along these lines may be able to explain the bent structure of the bis(cyclopentadienyl)lanthanides.

To conclude this section, we return to a discussion of the three lowest lying empty orbitals in the bent structure. The HOMO-LUMO gap increases from 0.01 eV in D<sub>5d</sub> to 0.16 eV in C<sub>2v</sub> symmetry. This is accompanied by a change

(33) Fischer, E. O.; Fischer, H. *J. Organomet. Chem.* **1965**, *3*, 181.  
 (34) Hayes, R. G.; Thomas, J. L. *Inorg. Chem.* **1969**, *8*, 2521. Thomas, J. L.; Hayes, R. G. *J. Organomet. Chem.* **1970**, *23*, 487.

(35) Ortiz, J. V.; Hoffman, R. *Inorg. Chem.* **1985**, *24*, 2095.

(36) Rittner, E. S. *J. Chem. Phys.* **1951**, *19*, 1030.

(37) Hildenbrand, D. L. *J. Electrochem. Soc.* **1979**, *126*, 1396.

(38) Drake, M. C.; Rosenblatt, G. M. *J. Electrochem. Soc.* **1979**, *126*, 1387.

(39) Guido, M.; Gigli, G. *J. Chem. Phys.* **1976**, *65*, 1397.

in symmetry of the LUMO,  $4a_{1g}$ . In  $C_{2v}$  symmetry, admixture of f-type partial waves to the LUMO, now  $a_1$ , is no longer symmetry-forbidden. The character of this orbital is s, 0.063, d, 0.076, and f, 0.066 (cf. Table II). The next two empty orbitals  $b_2$  and  $a_1$  derive from the  $3e_{2g}$  level; they undergo hardly any rehybridization due to bending. Contour maps reveal the shape of these orbitals as being rather similar to those of the extended Hückel orbitals.<sup>35</sup> Lanthanide d orbitals seem to be rather insensitive to changes in the ring-Ln-ring angle, unlike the transition-metal d orbitals which calculations indicate to undergo strong hybridization with metal s and p orbitals upon bending.<sup>8</sup>

### 3.2. Bis(pentamethylcyclopentadienyl)europium.

Though the structure of  $\text{Eu}(\text{C}_5\text{Me}_5)_2$  is unknown, it is reasonable to assume that it also is bent. However, from the results obtained for  $\text{Yb}(\text{C}_5\text{H}_5)_2$ , it seemed sufficient to perform the calculation on  $\text{Eu}(\text{C}_5\text{H}_5)_2$ , only for the  $D_{5d}$  structure with parallel rings.

An important difference between the Yb and the Eu complex is provided by the  $s^0f^7$  configuration of divalent europium. The half-filled shell of highly localized f electrons is expected to cause large spin polarization effects. Therefore a spin-polarized  $X\alpha$ -SW calculation<sup>15,32</sup> is mandatory to model the exchange interactions of the unpaired f electrons properly. However, due to the highly ionic character of the compound, spin polarization affects only the 4f ligand field manifold. All other levels, being quite delocalized over the molecule, shift very little upon spin polarization (about 0.1 eV upward). The exchange induced downward shift of the 4f orbitals by +0.53 to -2.90 eV produces the correct ground state with a HOMO-LUMO gap of 0.23 eV ( $4e_{1u}$  to  $4a_{1g}$ ). The corresponding transition-state excitation energy is 1.49 eV (850 nm), somewhat smaller than in  $\text{Yb}(\text{C}_5\text{H}_5)_2$ .

Overall the results for  $\text{Yb}(\text{C}_5\text{H}_5)_2$  and  $\text{Eu}(\text{C}_5\text{H}_5)_2$  are rather similar. The levels of  $\text{Eu}(\text{C}_5\text{H}_5)_2$  lie at somewhat higher energies than those in  $\text{Yb}(\text{C}_5\text{H}_5)_2$ , shifts reaching up to 0.3 eV for the cyclopentadienyl orbitals  $3a_{1g}$  to  $3e_{1u}$ . The Eu 4f manifold is slightly less localized. This is most apparent from the f partial wave occupation in the  $4e_{1u}$  orbital (0.925 vs. 0.940 in Yb; note the larger Eu sphere). The total partial wave populations in the metal sphere are quite similar for both compounds with a small but definitely larger covalency contribution of Eu p orbitals (see Table III). From the charge fractions in the central sphere one derives a charge of +1.34 for Yb, but only +1.06 for Eu.

The similarity of the findings for the two bis(cyclopentadienyl) complexes is in striking contrast to the results obtained for the lanthanide trihalides,  $\text{LnX}_3$ .<sup>18</sup> There, strong changes have been observed within one class of compounds when moving across the lanthanide series. Most noticeable is the position of the 4f manifold with respect to the ligand derived Ln-X  $\pi$ -bonding levels. For early lanthanide trihalides the 4f levels lie above the first ligand band, but they fall below these levels toward the end of the series. From the present calculations one is led to conclude that the 4f levels of the divalent lanthanides do not change their energy with respect to the ligand levels.

**3.3. Photoelectron Spectra.** Above an IE of 9 eV the He I and He II spectra of all three bis(pentamethylcyclopentadienyl)lanthanides are very similar; the complete spectrum of  $\text{Eu}(\text{C}_5\text{Me}_5)_2$  is shown in Figure 1. They also resemble that of other decamethylmetallocenes<sup>27</sup> though a shift to lower ionization energies of key features of about 0.3 eV is observed for the lanthanide complexes compared with  $\text{Fe}(\text{C}_5\text{Me}_5)_2$ .

Table V. States Arising in Ionization from  $f^n$  Free-Ion Configurations with First-Order Spin-Orbit Coupling<sup>13a</sup>

initial state	final state		multiplet components			
	LS	intensity	J	intensity	energy, eV	
$f^6 \ ^7F_0$	$^6H$	3.143	5/2	0.898	0	
			7/2	2.245	0.13	
	$^6F$	2.000	5/2	1.428	0.87	
			7/2	0.571	0.97	
	$^6P$	0.857	5/2	0.816	2.97	3.42 <sup>b</sup>
$f^7 \ ^8S_{7/2}$	$^7F$	7.000	0	0.143	0	
			1	0.429	0.028	
			2	0.714	0.084	
			3	1.000	0.168	
			4	1.286	0.280	
			5	1.571	0.419	
$f^{14} \ ^1S_0$	$^2F$	14.000	7/2	8.000	0	
			5/2	6.000	1.27	

<sup>a</sup> Only multiplet components with normalized intensity greater than 0.1 are listed. Energies relative to the ground state of the  $f^{n-1}$  ion are also given.<sup>14</sup> <sup>b</sup> The  $^6P_{5/2}$  state mixes strongly with the  $^4D_{5/2}$  state.

In the lower IE region, below 9 eV, the spectra differ from one another on account of the different patterns formed by the f bands. The spectra in this region are shown in Figures 2-4. In addition to the f bands, the ionizations from the top  $\pi$ -levels of the pentamethylcyclopentadienyl groups are expected here. There are various aids for disentangling the two types of ionization bands. First, 4f PE bands are of very low intensity when ionized by He I radiation but show substantial intensity increases relative to carbon 2p bands when the radiation is changed to He II.<sup>40</sup> Secondly, we have a clear expectation of the pattern of bands corresponding to the accessible ion states. The band intensities of the accessible states are predicted by Cox's rules<sup>13</sup> (see Table V). Their relative energies are expected to vary very little from those found in other lanthanide(III) compounds as the f orbitals are affected minimally by the ligand field.<sup>14</sup> The energy separations are also given in Table V.

**3.3.1.  $\text{Yb}(\text{C}_5\text{Me}_5)_2$ .** In the case of the Yb(II) compound which has an  $f^{14}$  configuration and a  $^1A_1$  ground state, the f ionization pattern is expected to be particularly simple; two ion states are accessible, namely,  $^2F_{7/2}$  and  $^2F_{5/2}$ , the former being the lower in energy. The first band in the spectrum at 6.1 eV is assigned to the  $^2F_{7/2}$  state as it shows a strong increase in relative intensity in the He II spectrum. The other f ionization is predicted to lie within the broad band centered at ca. 7.4 eV but cannot be distinguished in either the He I or the He II spectrum. The presumed position of this second  $^2F_{5/2}$  band is displayed in Figure 2. The ring ionizations are shown to dominate the band shape in the He I spectrum. There is no evident splitting into two main components as is found for the transition-metal metallocenes.

**3.3.2.  $\text{Sm}(\text{C}_5\text{Me}_5)_2$ .** In the case of the Sm(II) complex, where the molecule has a  $f^6$  configuration and a  $^7F_0$  ground state, the f-band spectrum is expected to be much more complex. It may well be also complicated by the fact that at the temperature of the experiment (ca. 115 °C) the  $^7F_1$  state may also be thermally populated. As in the case of the Yb complex, the first PE band may be definitively identified as an f band by its intensity characteristics (see Figure 3). Other predicted ionizations lie at the onset of the band centered on 7 eV and to higher IE of it. There

(40) Green, J. C.; Payne, M. P.; Seddon, E. A.; Andersen, R. A. *J. Chem. Soc., Dalton Trans.* 1982, 887.



**Table VI. Relative Band Areas for the Cyclopentadienyl (Cp) Uppermost Ring Ionizations and the f Bands for Ln(C<sub>5</sub>Me<sub>5</sub>)<sub>2</sub> (Ln = Sm, Eu, and Yb)**

photon energy	compd (n)	f band	f/n	Cp band n = 8	Cp/n	He II/He I
He I	Sm (6)	0.65	0.11	8	1	9
He II		5.92	0.99	8	1	
He I	Eu (7)	1.13	0.16	8	1	4.4
He II		4.92	0.70	8	1	
He I	Yb (14)	1.44	0.10	8	1	6.6
He II		9.21	0.66	8	1	

is evidence of the latter low intensity bands in the He II spectrum. Some structure is detectable on the 7-eV band, but again there is no significant splitting.

**3.3.3. Eu(C<sub>5</sub>Me<sub>5</sub>)<sub>2</sub>.** In the case of the Eu compound, the PE spectrum shows no resolved f band (see Figure 4). Thus the f ionization can be assumed to form part of the band that stretches from ca. 6 to 8 eV. Comparison of the position of the leading edge of this band with the comparable bands in the PE spectra of the Sm and Yb complexes suggests that the f ionization lies in the lower IE region of this band. The f band should consist of the seven *J* components of the <sup>7</sup>F state. In the fitting procedure, the shoulder at 6.3 eV was fitted exclusively by f-band onset, which gave an onset to the cyclopentadienyl band of ca. 6.5 eV, a value not dissimilar from that of the Yb and Sm compounds.

**3.3.4. Band Intensities.** The spectra were fitted with symmetric and asymmetric Gaussian curves, under the constraints indicated in the experimental section, in order to estimate the relative intensities of the f bands and the cyclopentadienyl bands in the He I and He II spectra. The results obtained are given in Table VI. The results have been normalized to an area of 8 for the cyclopentadienyl bands, and the areas are expressed both on this scale and also as the area per ionizing electron to enable comparison between the different lanthanides. The f bands show relative intensity increases of four-(Eu), seven-(Yb), and nine-(Sm) fold; though as the Eu band is unresolved, there must be a degree of uncertainty about this datum.

**3.3.5. Comparison with the Calculation.** The only quantitative criterion to judge the adequacy and accuracy of the present model calculations is a comparison with the PE spectra of the Yb and Eu complexes.

The experimental IEs have to be compared with the appropriate transition-state orbital energy (TSOE) to account for the various relaxation effects. For Yb(C<sub>5</sub>H<sub>5</sub>)<sub>2</sub> all transition-state calculations reported below have been performed in C<sub>2v</sub> geometry. However, TSOE results are as similar as the corresponding ground-state spectra. Therefore PE spectra may not be employed to differentiate

the two geometrical structures. In order to simplify the presentation of our results, only appropriately average energies labeled with D<sub>5d</sub> symmetry representations will be presented. For Eu(C<sub>5</sub>H<sub>5</sub>)<sub>2</sub>, spin-polarized transition-state calculations in D<sub>5d</sub> symmetry have been performed.

All ligand-derived orbitals for which transition states have been computed (2a<sub>1g</sub> to 3e<sub>1u</sub>) show a rather uniform relaxation of 2.19 ± 0.04 and 2.11 ± 0.01 eV for the Yb and Eu compounds, respectively. The 4f manifold, 3e<sub>2u</sub> to 4e<sub>1u</sub>, on the other hand, undergoes a significantly larger relaxation of 3.78 and 3.68 eV in Yb(C<sub>5</sub>H<sub>5</sub>)<sub>2</sub> and Eu(C<sub>5</sub>H<sub>5</sub>)<sub>2</sub>, respectively. This higher relaxation reflects rather directly the larger self-energy correction for the spatially compact f orbitals. The differing relaxation behavior reduces the gap between the f manifold and the center of the C-C levels, e<sub>1g</sub> and e<sub>1u</sub> from 2.44 eV in the X<sub>α</sub> ground-state spectrum of Yb(C<sub>5</sub>H<sub>5</sub>)<sub>2</sub> to 0.8 eV in the transition-state spectrum (and from 2.33 to 0.82 eV for Eu(C<sub>5</sub>H<sub>5</sub>)<sub>2</sub>). This is in fair agreement with the experimental values of 1.0 and 0.6 eV for Yb and Eu compounds, respectively. Calculated TSOE and peak energies are given in Table IV.

In comparing the experimental and calculated values for the ionization energies, we must take cognizance of the fact that the calculations are on the unmethylated derivatives. Sufficient data are available on unsubstituted and permethylated cyclopentadienyl complexes to give a good estimate of the likely shift in IE on permethylation.<sup>27</sup> The cyclopentadienyl upper levels shift more (1.5 eV) than the metal levels (1.0 eV). If we correct the calculated values by this amount, we obtained the estimated ionization energies given in Table VII. The estimates are somewhat low (a phenomenon typical for X<sub>α</sub>-SW results<sup>15,22</sup>), but the splitting pattern reproduces the experimental data well.

Particularly notable is the small predicted split in the ring e<sub>1</sub> bands. The PE bands of the d block decamethylmetallocenes show separate e<sub>1u</sub> and e<sub>1g</sub> ionization bands with differing He I/He II intensity ratios. The separation varies along the first transition series (V, 0.42 eV; Cr, 0.62 eV; Mn, 0.69 eV; Fe, 0.77 eV) as does the onset of the e<sub>1u</sub> band (V, 7.0 eV; Cr, 7.1 eV; Mn, 7.1 eV; Fe, 7.3 eV). The e<sub>1g</sub> orbitals have a covalent interaction with the metal 3d<sub>xz</sub> and 3d<sub>yz</sub> orbitals that increases along the first transition series; the e<sub>1u</sub> have as a symmetry partner the metal 4p<sub>x</sub> and 4p<sub>y</sub> orbitals that lie somewhat high in energy so the interaction is much less, and the e<sub>1u</sub>/e<sub>1g</sub> splitting increases along the series. The onset of the e<sub>1u</sub> band reflects the charge on the ring and is lowest for the most ionic member of the series, namely, V(C<sub>5</sub>Me<sub>5</sub>)<sub>2</sub>. For the lanthanide analogues, no splitting of the cyclopentadienyl band originating from the ring e<sub>1</sub> levels is observed. This may in part be due to the lower symmetry as the degeneracy of the e<sub>1</sub> levels is lifted. However, in the PE spectrum of stannocene, two bands are clearly resolved.<sup>41</sup> We,

**Table VII. Calculated Transition-State Orbital Energies (TSOE) (eV) for Ln(C<sub>5</sub>H<sub>5</sub>) and Estimated and Experimental Ionization Energies (IE) (eV) for Ln(C<sub>5</sub>Me<sub>5</sub>)<sub>2</sub> (Ln = Yb and Eu)**

type of bonding	orbital	Yb(C <sub>5</sub> H <sub>5</sub> ) <sub>2</sub> <sup>a</sup>	Yb(C <sub>5</sub> Me <sub>5</sub> ) <sub>2</sub>		Eu(C <sub>5</sub> Me <sub>5</sub> ) <sub>2</sub>		Eu(C <sub>5</sub> H <sub>5</sub> ) <sub>2</sub> <sup>b</sup>
		TSOE	estd <sup>c</sup> IE	exptl IE	estd <sup>c</sup> IE	exptl IE	TSOE
π-C-C	Ln f	6.91 <sup>d</sup>	5.9	6.7 <sup>e</sup>	5.6	6.4 <sup>e</sup>	6.60 <sup>d</sup>
	3e <sub>1u</sub>	7.63	6.2	7.2 (A <sub>2</sub> )	5.9	6.9 (A <sub>2</sub> , A <sub>3</sub> ) <sup>f</sup>	7.26
	3e <sub>1g</sub>	7.79					7.57
π-C-C	3a <sub>2u</sub>	11.11	9.6	10.1 (B <sub>1</sub> )	9.3	9.8 (B <sub>1</sub> )	10.75
	3a <sub>1g</sub>	11.61	10.1	10.9 (B <sub>2</sub> )	9.7	10.5 (B <sub>2</sub> )	11.20
σ-C-H	2e <sub>2u</sub>	12.40	10.9	12.0 (B <sub>3</sub> )	10.8	11.6 (B <sub>3</sub> )	12.29
σ-C-C	2e <sub>1u</sub>	12.74	11.2	13.8 (B <sub>4</sub> )	10.9	13.4 (B <sub>4</sub> )	12.43

<sup>a</sup> Calculation with tilted rings (C<sub>2v</sub> symmetry). <sup>b</sup> Spin-polarized calculation. <sup>c</sup> TSOEs for Ln(C<sub>5</sub>H<sub>5</sub>)<sub>2</sub> uniformly reduced by 1.5 eV (Ln f energy reduced by 1.0 eV only). <sup>d</sup> Average over f manifold. <sup>e</sup> Spin-orbit average using the fitting results. <sup>f</sup> Average energy of bands A<sub>2</sub> and A<sub>3</sub>.



**Table VIII. Comparison of Atomic Ionization Energies (eV) for the Process  $\text{Ln}^{2+} \rightarrow \text{Ln}^{3+} + e^-$  with f Orbital Ionization Energies (eV) of  $\text{Ln}(\text{C}_5\text{Me}_5)_2$**

	$\text{Ln}^{2+}$			
	$\text{Ln}(\text{C}_5\text{Me}_5)_2$			
	TSEO	exptl <sup>a</sup>	TSEO <sup>b</sup>	exptl
Yb	25.3	25.2	5.9	6.65 <sup>c</sup>
Eu	25.1 <sup>d</sup>	24.9	5.6 <sup>d</sup>	6.42 <sup>c</sup>
(Yb-Eu)	0.2	0.3	0.3	0.2

<sup>a</sup>References 42 and 43. <sup>b</sup>Estimated values; see Table VII. <sup>c</sup>Spin-orbit average using the results of the fit. <sup>d</sup>Spin-polarized calculated.

therefore, attribute the lack of structure to the highly ionic nature of this complex, revealed by the calculations. The onset of the ring ionizations lies considerably lower than those given above (Sm, 6.3 eV; Eu, 6.3 eV; Yb, 6.5 eV), reinforcing the view that the rings of the lanthanide complexes are more negatively charged as indicated by the calculations.

Concomitant with the type of ionic behavior found by both calculation and experiment is a rather corelike be-

havior of the 4f electrons. A stringent test of the validity of our calculation procedure for the f ionizations is to calculate the IE of the corresponding  $\text{Ln}^{2+}$  ions. In Table VIII we compare experimental data for the processes  $\text{Yb}^{2+} (f^{14} \rightarrow f^{13})^{42}$  and  $\text{Eu}^{2+} (f^7 \rightarrow f^6)$ , the latter value being obtained from a Born-Haber procedure,<sup>43</sup> and the appropriate TSEO from atomic  $X\alpha$  calculations, to calculated and spin-orbit averaged IEs of the bis(pentamethylcyclopentadienyl) sandwich compounds. Calculated and experimental atomic ionization energies agree very well, as do the values for the complexes. This adds weight to the assignment of the Eu f band to the low-energy shoulder at 6.3 eV.

**Acknowledgment.** This work has been supported by the Deutsche Forschungsgemeinschaft, the Fonds der Chemischen Industrie, and the SERC. We also wish to acknowledge the collaboration of R. A. Andersen, J. M. Boncella, and C. J. Burns.

**Registry No.**  $\text{Sm}(\text{C}_5\text{Me}_5)_2$ , 90866-66-3;  $\text{Eu}(\text{C}_5\text{Me}_5)_2$ , 101200-04-8;  $\text{Yb}(\text{C}_5\text{Me}_5)_2$ , 75764-11-3;  $\text{Eu}(\text{C}_5\text{H}_5)_2$ , 1271-25-6;  $\text{Yb}(\text{C}_5\text{H}_5)_2$ , 1271-31-4.

(42) *CRC Handbook of Chemistry and Physics*, 61st ed.; CRC Press: Boca Raton, 1980.

(43) Faktor, M. M.; Hanks, R. J. *Inorg. Nucl. Chem.* 1969, 31, 1649.

(41) Cradock, S.; Duncan, W. J. *Chem. Soc., Faraday Trans. 2* 1978, 74, 194.

## Decomposition Mechanism and Kinetics of *n*-Butylsilane

B. A. Sawrey, H. E. O'Neal,\* and M. A. Ring\*

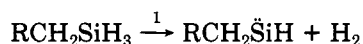
Department of Chemistry, San Diego State University, San Diego, California 92182

Received July 29, 1986

The thermal decomposition kinetics of *n*-butylsilane have been studied at 4800 torr between 1085 and 1250 K. Overall rate constants below 1150 K compare closely to those of other monoalkylsilanes but become increasingly larger at higher temperatures. The dominant primary dissociation processes are 1,1- and 1,2- $\text{H}_2$  eliminations (in the ratio of  $2.1 \pm 0.6$ , respectively); C-C bond fissions also contribute at the higher temperatures. Silylene chain reactions as well as short free-radical chains occur in the uninhibited reaction. The dominant reaction intermediate, *n*-butylsilylene, decomposes to a variety of olefin products and also isomerizes to silacyclopentane via an intramolecular silylene insertion into C-H bonds of the end methyl group. Observation of this product supports the consecutive step mechanism for the decompositions of alkylsilylenes ( $R > \text{Me}$ ), i.e., intramolecular silylene insertion into C-H bonds to produce silacyclic compounds followed by their subsequent decompositions to various olefins and silylenes (or silenes).

### Introduction

The shock-induced decompositions of monoalkylsilanes<sup>1-4</sup> (1085-1250 K) occur mainly by two primary dissociation channels, 1,1- $\text{H}_2$  elimination and 1,2- $\text{H}_2$  elimination (reactions 1 and 2), with the former being the more



important by factors of 2-5. A third primary process, namely, alkane elimination, has also been observed for

(1) Davidson, I. M. T.; Ring, M. A. *J. Chem. Soc., Faraday Trans. 1* 1980, 76, 1520. Sawrey, B. A.; O'Neal, H. E.; Ring, M. A.; Coffey, D. *Int. J. Chem. Kin.* 1984, 16, 31.

(2) Rickborn, S. F.; Ring, M. A.; O'Neal, H. E. *Int. J. Chem. Kinet.* 1984, 16, 1371.

(3) Sawrey, B. A.; O'Neal, H. E.; Ring, M. A.; Coffey, D. *Int. J. Chem. Kinet.* 1984, 16, 801.

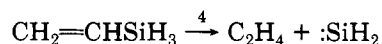
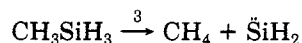
(4) Rickborn, S. F.; Ring, M. A.; O'Neal, H. E.; Coffey, D. *Int. J. Chem. Kinet.* 1984, 16, 289.

**Table I. Monoalkylsilane Decomposition Kinetic Parameters**

compd	log A	E, kcal	$k_H/k_D$	$\phi_{1,1}/\phi_{1,2}$	$k_{1145^\circ\text{C}}/s^{-1}$
$\text{CH}_3\text{SiH}_3^1$	15.29 <sup>a</sup>	65 015 ± 3000 <sup>a</sup>	1.1	4.7	757
$\text{CH}_3\text{CH}_2\text{SiH}_3^2$	15.14	64 769 ± 940	1.23	2.2	597
$\text{CH}_2=\text{CHSiH}_3^4$	14.95	63 268 ± 1259	1.29		746
$\text{CH}_3\text{CH}_2\text{CH}_2\text{SiH}_3^3$	15.26	65 300 ± 1950		3.0	624

<sup>a</sup>High-pressure parameters obtained via RKKM fall-off corrections.

methylsilane (reaction 3)<sup>1</sup> and vinylsilane<sup>4</sup> (reaction 4), but curiously not for ethylsilane<sup>2</sup> and propylsilane.<sup>3</sup>



The kinetics of the monoalkylsilane decompositions show many similarities. Thus, the overall Arrhenius pa-